International Journal of the Korean Society of Precision Engineering, Vol. 3, No. 3. July 2002.

Trajectory Following Control Using Cogging Force Model in Linear Positioning System

Myung-Jin Chung[1] and Dae-Gab Gweon[2]

[1] Department of Mechanical Engineering, KAIST, Taejon, South Korea
[2] Department of Mechanical Engineering, KAIST, Taejon, South Korea

ABSTRACT

To satisfy the requirement of the one axis linear positioning system, which is following control of the desired trajectory without following error and is the high positioning accuracy, feed-forward loop having cogging force model is proposed. In the one axis linear positioning system with linear PM motor, cogging force acting as disturbance is modeled analytically. Analytic model of cogging force is verified by result measured from positioning system constructed with linear PM motor. Measured result is very similar with proposed analytic model. Cogging force model is used as feed-forward loop in control scheme of linear positioning system. Cogging force feed-forward loop is obtained from analytic model of cogging force. Trajectory following error is reduced from 300nm to 100nm by applying the proposed cogging force feed-forward loop. By using analytic model of cogging force, the control scheme is simplified. Also this analytic model is applicable to calculation of characteristic value of positioning system in design process.

Keywords : Linear positioning system, Cogging force model, Trajectory following control, Feed-forward Control, Linear brushless permanent magnet motor

1. Introduction

There is an increasing requirement for controlling linear motion from several ten nanometers to a few hundred of millimeter strokes in the area of the semiconductor industries and the precision manufacturing. Linear positioning system with direct driving method such as piezoelectric drive and permanent magnet (PM) motor could offer significant advantages over conventional linear actuation technologies[1,2]. Among these direct driving methods, linear PM motor is a proper method for long stroke and high accuracy. Linear PM motor has significant advantages over conventional linear actuation technologies, such as motors driven by cams, linkages and pneumatic rams, in terms of efficiency, operating bandwidth, speed and thrust control, stroke and positioning accuracy with low kinematical complexity.

The requirement of the one axis linear positioning system is following control of the desired trajectory without following error and is the high positioning accuracy. To satisfy these performances, the design and control methodologies are proposed in many researches, such as current harmonic injection techniques based on open-loop cancellation[3], feedback control techniques using the estimator and observer[4], and the neural network-based controllers[5]. But these methods have some limitations; 1) Back-emf is required for calculation of current shape, 2) Controller is complex by using the estimator and observer, 3) Learning process is required for neural network application.

Therefore, in this work cogging force acting as disturbance of linear PM motor is modeled analytically. Analytic model of cogging force is verified by result measured from positioning system constructed with linear PM motor. Measured result is very similar with proposed analytic model. Cogging force model is used as feed-forward loop in control scheme of linear positioning system. Cogging force feed-forward loop is obtained

from analytic model of cogging force. Trajectory following error is reduced from 300nm to 100nm by applying the proposed cogging force feed-forward loop. Also this analytic model is applicable to calculation of characteristic value of positioning system in design process.

2. Cogging Force Model

2.1 System Configuration

The linear positioning system consists of two linear PM motors, one square air bearing and moving stage as in Fig. 1. Table 1 lists the specifications of linear positioning system.

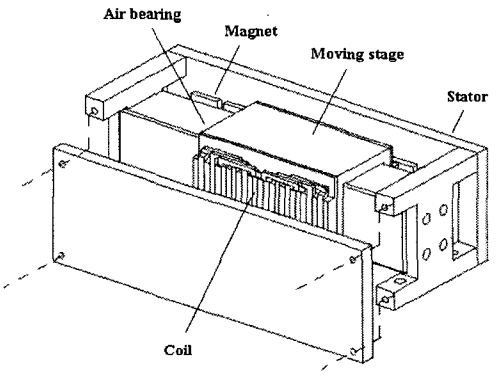

Fig. 1 Configuration of linear positioning system

Table 1 Specifications of linear positioning system

Item		Value	Unit
Linear motor	Number of phase	3	-
	Pole pitch	24.0	mm
	Number of pole	6	-
	Magnet height	3.0	mm
	Magnet width	18.0	mm
	Air gap length	3.0	mm
	Slot width	4.0	mm
	Effective length	50.0	mm
	Remanence flux density	1.2	T
Air bearing	Stiffness	38	N/μm
	Max. Load	300	N

Two linear PM motors using brushless PM motor are attached to each side of air bearing slider symmetrically, and moving stage is fixed at upper side of slider. By virtue of symmetrical configuration, this system is robust to thermal variation, which is appropriate to precision system. Square air bearing is used to guide moving stage. Since the square air bearing slider tends to move to the center of guide cross section, the moving stage can move freely along the guide rail with little parasitic motion. Due to the characteristics of air bearing, the positioning system has little friction and wear, so precise and smooth motion control is possible.

2.2 Analytic Model of Cogging Force

Force components can be represented as the function of geometric and electric parameters of linear PM motor with analytic model. As in Fig. 1, the linear positioning system has actuating method with two linear PM motors and guiding method with one square air bearing. The dynamic equation of the linear positioning system is represented as

$$m\ddot{x}+b\dot{x}+kx=F_{act}=F_c+F_{drv} \tag{1}$$

where F_{act} is actuating force of positioning system, F_{drv} is driving force generated by air gap flux density and current, and F_c is a cogging force generated by PM and iron core of armature and acts as disturbance force of PM motor. Due to the characteristics of air bearing, damping (b) and stiffness (k) of linear positioning system can be neglected along the moving direction.

In the linear PM motor, actuating force consisted of cogging force and driving force as in Eq. (1) and each force can be calculated analytically.

The cogging force acting on iron core of armature of PM motor is obtained by Maxwell stress tensor method, which integrates the no load flux density along the slot face on the iron core of armature. This force is given by

$$F_c=\frac{l_e}{2\mu_0}\int(B_n^2-B_t^2)dl \tag{2}$$

where μ_0 is magnetic permeability of air and B_n and B_t are normal and tangential component of flux density.

In linear PM motor, the cogging force has two components, which are end-effect ripple and tooth ripple, as shown in Fig. 2. The end-effect ripple component is

calculated at the two end sides of iron core of armature and given by

$$F_e(x_0) = -F_{e\_f}(x_0) + F_{e\_r}(x_0) \tag{3}$$

where x_0 is a relative position of stator and armature.

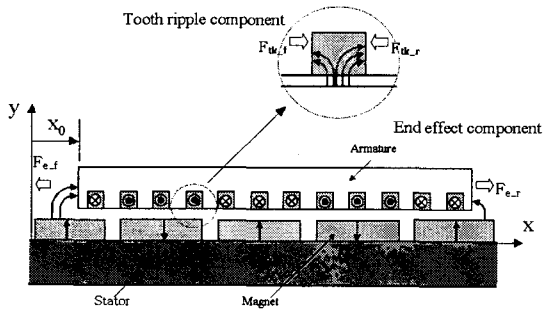

Fig. 2 Cogging force components

The tooth ripple component is calculated by summation of force acting at each slot areas with two sides and given by

$$F_t(x_0) = \sum_{k=1}^{Q_s} \{F_{tk\_f}(x_0) - F_{tk\_r}(x_0)\} \tag{4}$$

where Q_S is number of slot.

The driving force can be obtained by summation of static thrust of the each phase and given by

$$F_{drv}(x_0) = nl_e \sum_{p=1}^{3} B_p i_p \tag{5}$$

where n is number of coil turn, l_e is effective length, B_p is air gap flux density, and i_p is winding coil current, respectively.

Fig. 3 shows the cogging force, which is analytically calculated with 0.2mm step by using Eq. (3)-(4).

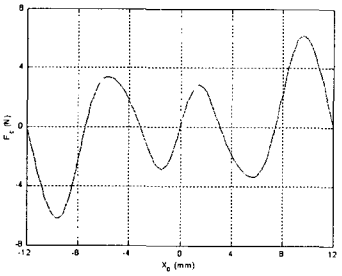

Fig. 3 Calculated cogging force

In each equations, the flux density equation obtained by magnetic field analysis[6] is used and given by

$$B(x) = \alpha_s \sum_{n=1,3,5,..}^{\infty} \beta_s \left(e^{\frac{2n\pi h_M}{\tau_p}} e^{\frac{n\pi\delta}{\tau_p}} + e^{\frac{n\pi\delta}{\tau_p}}\right) \cos\frac{n\pi x}{\tau_p} \tag{6}$$

where

$\alpha_s = -f(\mu_M, \delta, h_M)$ and $\beta_s = f(B_r, \alpha, \delta, \tau_p, \mu_M, \mu_0, h_M)$ for $(k-1)\tau_S - w_s/2 \le x \le (k-1)\tau_S + w_s/2$ in k=1, 2, 3, ... Q_S and μ_M is magnetic permeability of PM, δ is air gap length, h_M is magnet height, B_r is remanence flux density of magnet, α is ratio of magnet length to pole pitch, τ_p is pole pitch, and w_S is slot width, respectively.

3. Feed-forward Control Loop Model

The general feedback control scheme of positioning system is shown in Fig. 4. The cogging force acts as disturbances and control input saturated by driver circuit.

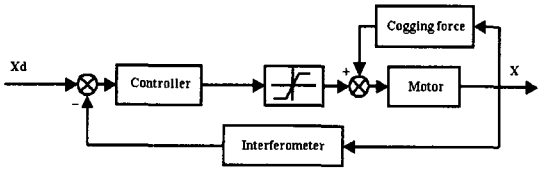

Fig. 4 Block diagram of feedback control loop

In order to reject the cogging force appearing in positioning system, the feed-forward loop is adopted in general feedback control loop as shown in Fig. 5.

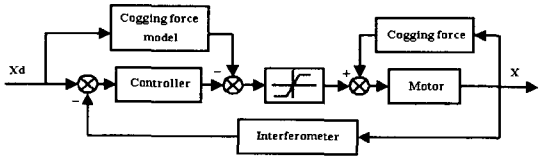

Fig. 5 Block diagram of cogging force feed-forward loop

The cogging force depends on relative position of armature and magnet and is independent with current flow. The cogging force calculated from Eq. (3)-(4) can be described in the form of Fourier series as given by

$$F_c(x_0) = cr_0 + \sum_{k=1}^{n} \left(cr_k \cos\frac{k\pi x_0}{\tau} + ci_k \sin\frac{k\pi x_0}{\tau}\right) \tag{7}$$

where cr_0, cr_k and ci_k are coefficients of Fourier series.

From Eq. (7), cogging force model is obtained and described as follows

$$v_c(x_0) = K_c(x_0)\{cr_0 + \sum_{k=1}^{n}(cr_k \cos\frac{k\pi x_0}{\tau} + ci_k \sin\frac{k\pi x_0}{\tau})\} \quad (8)$$

where K_c is cogging force conversion factor from cogging force to voltage.

4. Trajectory Following Control

4.1 Verification of the Cogging Force

To verify the cogging force model, measurement of cogging force is conducted in linear positioning system, which is constructed with linear PM motor, air bearing and moving stage. Fig. 6 shows the experimental setup, where the position is measured by laser interferometer (HP10706A) and force components are measured by load cell (BCL-30L).

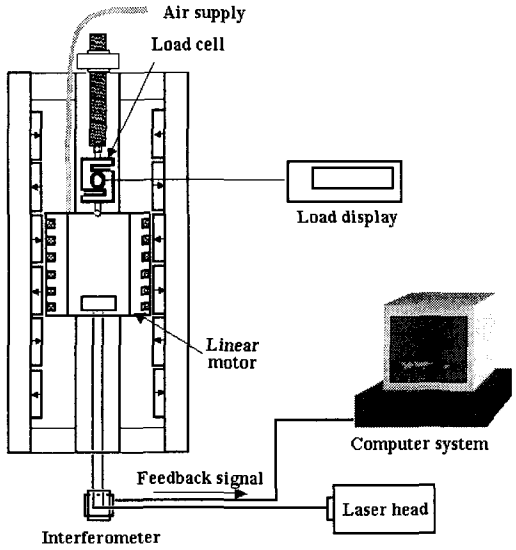

Fig. 6 Experimental setup for cogging force measurement

In this setup, the armature is fixed on air bearing slider and guided along air bearing guide rail. One leg of the load cell is coupled to moving stage and the other leg is fixed on the lead screw. By changing the relative position of armature and stator, the leg of the load cell is compressed or extended. The amount of compression or extension depends on the magnitude of cogging force.

Fig. 7 shows the cogging force, which is measured without current input with 1mm step. Fig. 8 shows the Fourier coefficients of each cogging force, which are calculated from Fig. 3 and Fig. 7. In Fourier coefficients, cr_1, cr_2, cr_4 ... and ci_1, ci_2, ci_4 ... represent coefficients of end effect components and cr_3, cr_6, cr_9 ... and ci_3, ci_6, ci_9 ... are coefficients of tooth ripple component.

The cogging force components are calculated from the Fourier coefficients of each cogging force as given by Eq. (9).

$$F_e(x_0) = \sum_{k=1,2,4,5,7...}^{n}(cr_k \cos\frac{k\pi x_0}{\tau} + ci_k \sin\frac{k\pi x_0}{\tau}) \quad (9\text{-a})$$

$$F_t(x_0) = \sum_{k=3,6,9...}^{n}(cr_k \cos\frac{k\pi x_0}{\tau} + ci_k \sin\frac{k\pi x_0}{\tau}) \quad (9\text{-b})$$

where cr_k and ci_k are coefficients of Fourier series. Table 2 lists the cogging force component acting on the positioning system, where measured value is very similar with calculated value.

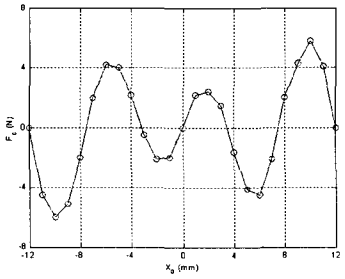

Fig. 7 Measured cogging force

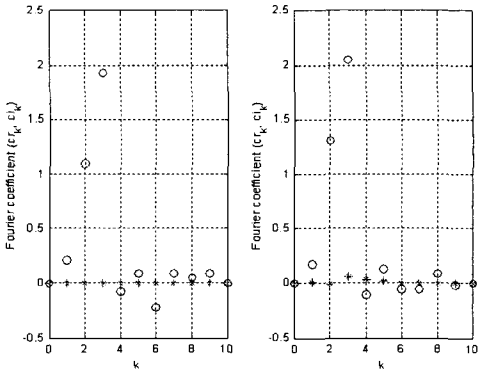

(a) (b)

Fig. 8 Fourier coefficients of cogging force: (a) Calculated cogging force (b) Measured cogging force, where * is cr_k and o is ci_k

Table 2 Comparison of cogging force components acting on the positioning system

Cogging force	Calculated	Measured	Unit
End-effect	2.6	2.7	N
Tooth	3.9	4.1	N

4.2 Effects of the Cogging Force in Positioning Control

The experimental setup for positioning control is shown in Fig. 9. In this setup, the motor driving signal is generated by pulse width modulation method and fed to winding coil via motor driver board using L298. The positioning sensor is a single beam laser interferometer (HP10706A) with the position resolution of 10nm. The control input is generated by PID controller as given by

$$v_{ci} = k_p\{(x_d - x) + k_d(\dot{x}_d - \dot{x}) + k_i\int(x_d - x)dt\} \qquad (10)$$

where k_p, k_d, k_i are PID gains and should be tuned properly.

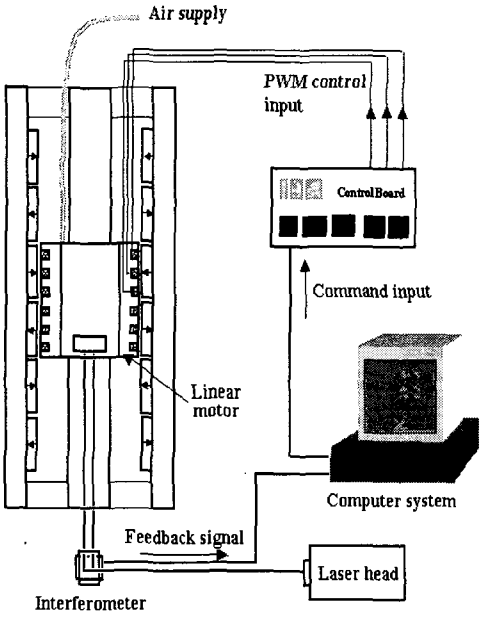

Fig. 9 Experimental setup for positioning control

The control input is driven to the three phase winding coils through control board according to relative position and given by

$$v_{ci\_a} = v_{ci}\cos\{\frac{2\pi(x+x_0)}{\tau}\}$$
$$v_{ci\_b} = v_{ci}\cos\{\frac{2\pi(x+x_0)}{\tau} + \frac{2\pi}{3}\}$$
$$v_{ci\_c} = v_{ci}\cos\{\frac{2\pi(x+x_0)}{\tau} + \frac{4\pi}{3}\} \qquad (11)$$

where v_{ci} is a control input generated by PID controller.

In order to show the effect of the cogging force in positioning control, 20mm step positioning control is conducted with linear positioning system. The step response of positioning system is shown in Fig. 10, where different transient fluctuating error of each step is showed by acting of different cogging force at each step motion. Different steady state control input value is acted to cancel out different cogging force at each step. Positioning error of steady state is measured to 50nm at each step. From the experiment of the step positioning control, Authors think that the cogging force has an effect on the transient fluctuating error but has little effect on the steady-state error.

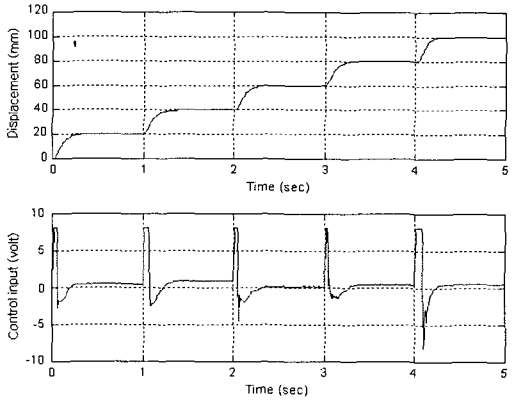

Fig. 10 Step response of positioning system

4.3 Trajectory Following Control without Feed-forward Loop

In order to show the trajectory following capability, 100mm trajectory following control is conducted with linear positioning system. The trajectory following response of positioning system is shown in Fig. 11.

At the constant velocity range of Fig. 11, control input is fluctuating with constant period to compensate disturbance of cogging force generated by PM motor. The fluctuating period of following error (six pick for 48mm during 2.4sec) is similar with that of measured

cogging force (three pick for 24mm as shown in Fig. 7). For the constant velocity range, maximum following error is appeared as 300nm.

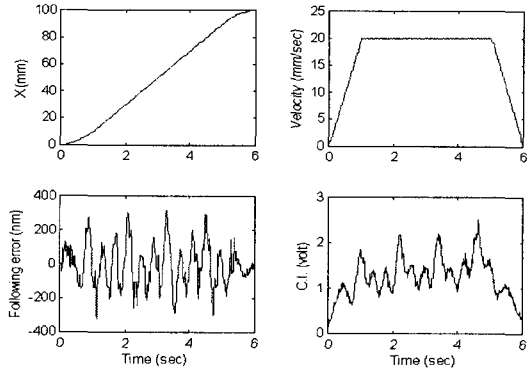

Fig. 11 Trajectory following control without feed-forward loop

From the experiment of the trajectory following control, authors think that the following error of trajectory following control affected by cogging force of positioning system and the trajectory following error does not suppressed perfectly by feedback control.

4.4 Application of the Cogging Force Model

From the trajectory following control of positioning system, there is limitation of following error suppression by feedback control. To reduce the error, feed-forward loop with cogging force model is adopted in feedback control scheme.

Fig. 12 shows the trajectory following response with cogging force model as feed-forward loop.

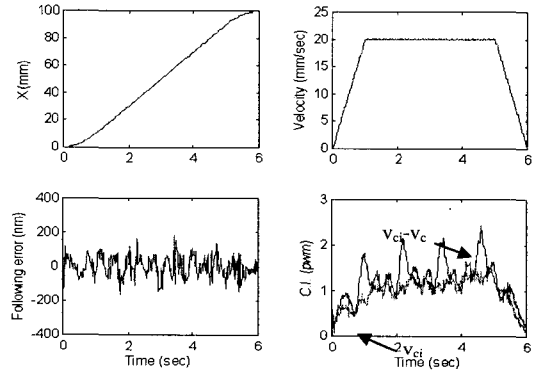

Fig. 12 Trajectory following control with feed-forward loop

In Fig. 12, the maximum following error is 100nm, where trajectory following error is improved if compared with response without feed-forward of cogging force model as in Fig. 11.

From the experiment of the trajectory following control with feed-forward loop, cogging force model is applicable to suppress effectively the following error.

5. Conclusions

To satisfy the requirement of the one axis linear positioning system, which is following control of the desired trajectory without following error and is the high positioning accuracy, feed-forward loop having cogging force model is proposed. In one axis linear positioning system with linear PM motor, cogging force acting as disturbance is modeled analytically. Analytic model of cogging force is verified by result measured from positioning system constructed with linear PM motor. Measured result is very similar with proposed analytic model. Cogging force model is used as feed-forward loop in control scheme of linear positioning system. Cogging force feed-forward loop is obtained from analytic model of cogging force. Trajectory following error is reduced from 300nm to 100nm by applying the proposed cogging force feed-forward loop. By using analytic model of cogging force, the control scheme is simplified. Also this analytic model is applicable to calculation of characteristic value of positioning system in design process.

Acknowledgement

Authors thank to Kim Kee-Hyun of KAIST for assistance of experiments.

References

1. Ryu, J. W. and Gweon, D. G., "The optimal design of a flexure hinge based xy-theta wafer stage," ASPE, Vol. 21, No. 1, pp. 18-28, 1997.
2. Lee, M. G. and Gweon, D. G., "CD/DVD compatible optical pickup actuator design," KSPE, Vol. 15, No. 7, pp. 98-103, 1998.
3. Braembussche, P. V. D. et al., "Accurate tracking control of linear synchronous motor machine tool

axes," Mechatronics, Vol. 6, No. 5, pp. 507-521, 1996.

4. Low, T. S. et al, "Servo performance of a BLDC drive with instantaneous torque control," IEEE Trans. on Industrial Application, Vol. 28, No. 2, pp. 455–462, 1992.
5. Otten, G. et al, "Linear motor motion control using a learning feedforward controller," IEEE/ASME Trans. on Mechatronics, Vol. 2, No. 3, pp. 179-187, 1997.
6. Chung, M. J. and Gweon, D. G., "Modeling of the armature slotting effect in the magnetic field distribution of a linear permanent magnet motor," Electrical Engineering, Vol. 84, No. 2, pp. 101–108, 2002.